International Journal of Environmental Science and Technology (2019) 16:1239–1248
https://doi.org/10.1007/s13762-018-1773-0

ORIGINAL PAPER

Silver nanoparticles in building materials for environment protection against microorganisms

G. D. da Silva[1] · E. J. Guidelli[2] · G. M. de Queiroz-Fernandes[1] · M. R. M. Chaves[1] · O. Baffa[2] · A. Kinoshita[1]

Received: 30 August 2017 / Revised: 28 January 2018 / Accepted: 11 May 2018 / Published online: 21 May 2018

Abstract

Gypsum and grout are finishing materials found in almost all constructions. Specifically, gypsum has been widely used because of its low cost in the composition of drywall. However, in humid environments, they are susceptible to microorganism infestation. In this work, silver nanoparticles (Ag-NPs) were incorporated to gypsum (643 and 321 ppm) and grout (227 ppm) and the antimicrobial activity tested. The MIC value for Ag-NPs solution was 26.8 μg ml^{-1} for *Staphylococcus aureus*, *Pseudomonas aeruginosa*, and *Escherichia coli* and 428 μg ml^{-1} for the *A. Niger*. Another MIC test with specimen component dilutions indicated that grout and gypsum do not exhibit antibacterial activity against *S. aureus*. However, when incorporated with Ag-NPs, both grout and gypsum demonstrate growth inhibition. In a biofilm test performed with *S. aureus*, SEM images revealed crenation of bacteria in contact with specimens containing Ag-NPs. The addition of Ag-NPs causes change in color that was measured through CIELAB (International Commission on Illumination) color coordinates. There is no difference in the *L* value parameter (lightness) for all materials tested. However, the comparison between the parameters *a* (green–red coordinate) and *b* (blue–yellow) for gypsum and grout results in a statistically significant difference ($p < 0.05$, Kruskal). The values of *b* increase as the Ag-NPs concentration increases because of the yellowish coloration of the solution. It can be concluded that Ag-NPs can be incorporated to gypsum and grout, maintaining its antimicrobial feature improving the material properties, which can benefit health and the environment.

Keywords Microorganisms · Gypsum · Grout · *A. niger*

Introduction

Antibacterial, antifungal, and antiviral properties of silver (Ag) have long been known (Morones et al. 2005). Currently, silver nanoparticles (Ag-NPs) have been applied in many health areas due to their broad bactericidal spectrum and antiviral properties. They are effective against Gram-negative bacteria *E. coli, V. cholera, P. aeruginosa, and S. typhus* (Morones et al. 2005; Xie et al. 2014), and oral bacteria, such as *S. mutans* (Cheng et al. 2012) and Gram-positive *S. aureus* bacteria (Dos Santos et al. 2014). Some studies focus on the development of new drugs/materials able to combat resistant strains of microorganisms, which are a public health issue (He et al. 2011; Dos Santos et al. 2014; Ogar et al. 2015).

Colloidal solutions of metals, such as silver, gold, and zinc, are nanoscale systems whose particle sizes are in the range of 1 and 100 nm. They are particularly interesting because the synthesis processes are relatively simple, usually by means of reducing agents and surfactants, among others (Paschoalino et al. 2010; Guzman et al. 2012). Small changes in the shape and size of these nanoparticles can alter their characteristics such as surface area and agglomeration/dispersion capacity. In general, the smaller the particle size, the greater the antimicrobial effect (Rai et al. 2009; Ann et al. 2014).

One of the main difficulties in the synthesis of these metallic nanoparticles is to obtain stable colloidal suspensions, since they have a high surface energy that favors particle aggregation. To avoid particle aggregation,

Editorial responsibility: Agnieszka Galuszka.

✉ A. Kinoshita
angelamitie@gmail.com

[1] Universidade do Sagrado Coração, Rua Irmã Arminda 10-50, Bauru, São Paulo 17.011-160, Brazil

[2] Departamento de Física, FFCLRP, Universidade de São Paulo, Av Bandeirantes 3900, Ribeirão Prêto, São Paulo 14.900-000, Brazil

stabilizing polymers such as PVA (polyvinyl alcohol), PVP (polyvinylpyrrolidone), among others, are used so that the nanoparticles do not clump together (Guidelli et al. 2013). Ag-NPs synthesis methods involve the reduction of an ionic salt in the appropriate medium in the presence of reducing agents. The antimicrobial activity is influenced by the silver concentration in the solution (Guzman et al. 2012; Singh and Prasad 2016).

Literature reports several applications of Ag-NPs in health science due to their antimicrobial potential (Rai et al. 2009) and more recently in the control of *Aedes aegypti* (Suresh et al. 2015). Among the applications, one can mention their use in dressings (Maneerung et al. 2008; Abdelgawad et al. 2014) and in the production of new biomaterials (Liu et al. 2012; Guidelli et al. 2013). In environmental science, there are applications for bioremediation. Ag-NPs formed in situ on the surface of *S. cerevisiae* proved to be effective in the removal of heavy metals such as Cr, As, Pb, Cu, Mn, Zn, Hg, and Ni (Chen et al. 2017).

However, application in building materials is still little explored and reports in the literature are rare. Gypsum is hygroscopic and porous. This makes it retain moisture easily and quickly; however, its drying is slow. As such, it becomes a propitious site for fungal growth (Dedesko and Siegel 2015). The grout is composed of Portland cement, mineral aggregates, inorganic pigments, and other chemical additives. The conventional way of avoiding the proliferation of fungi in grout is through polymeric additives for waterproofing. However, it is known that the method is not fully efficient. Thus, adding an antimicrobial additive to the mixture would lead the grout to not only prevent the passage of water between ceramics, but also prevent the proliferation of microorganisms.

As mentioned by Ogar et al. 2015 and Bellotti et al. 2015, the control of infestation by fungi in indoor environments is important for the health of the inhabitants and Ag-NPs has potential application in this sense. Recently, Vesper et al. 2016 related the use of drywall to an increased incidence of asthma, due to the high susceptibility of this material to accumulate fungi. In addition, infestation by fungi on objects made with gypsum plaster may cause damage to objects with historical and cultural heritage, due to their deterioration (Jroundi et al. 2014).

This paper reports the induction/improvement of the antimicrobial activity of gypsum plaster and grout by the incorporation of Ag-NPs in their composition. Minimum inhibitory concentration tests were carried out for the nanoparticle solution, as well as for mixtures with gypsum and grout, demonstrating Ag-NP activity in the mixtures. Specimens of gypsum and grout made with Ag-NPs were tested against *S aureous* biofilm and filamentous fungus *A. niger*, demonstrating the efficacy of these new materials.

Materials and methods

Synthesis of Ag-NPs

Silver nanoparticles were synthesized by the method described elsewhere (Guidelli et al. 2013, 2014). Briefly, 1 ml of a PVA (polyvinyl alcohol) solution (1.25 g l^{-1}) was added to 25 ml of a silver nitrate solution (16 mM). A sodium borohydride solution ($NaBH_4$—32 mM) was then slowly added under vigorous stirring at room temperature 25 °C. The yellow color characteristic of spherical silver nanoparticles obtained at the end of the synthesis indicates the formation of stable nanoparticles. UV–Vis spectroscopy confirmed the synthesis of silver nanoparticles due to the presence of a plasmonic peak at 390 nm.

The characterization of Ag-NPs was performed through UV–Vis spectroscopy, dynamic light scattering (DLS), and transmission electron microscopy. The UV–Vis absorption spectra of the colloidal dispersions were recorded on an Ultrospec 2100 pro (Amersham Pharmacia) spectrophotometer. The solution concentration is 856 µg ml^{-1} of Ag^+. The average particle size was obtained by DLS, with the aid of a Zeta-Sizer system HS500 (Malvern Instruments) operating at a fixed wavelength (633 nm He–Ne laser) and angle (90°). Transmission electron microscopy images were recorded on a JEOL-JEM-CXII-10®, by drying a drop of the colloidal dispersions on a copper grid covered with a conductive polymer.

Specimen

For the experiments, the gypsum plaster (Qualigesso® 60′, Brazil) and grout (WeberQuartzolit®, Brazil) were previously sterilized with gamma radiation at dose of 25 kGy. All specimens were produced under sterile conditions.

The gypsum plaster and grout specimen were prepared according to the manufacturer's instructions. For the grout

samples, we used 37.7 g of cement associated with 10 ml of Ag-NPs dispersion resulting in a 227-ppm specimen (grout 100%). For gypsum, 13.3 g of gypsum powder was associated with 10 ml of Ag-NPs dispersion, resulting in a concentration of 643 ppm (gypsum 100%) and, in another preparation, 5 ml of Ag-NPs associated with 5 ml of water (Milli-Q) resulting in a 321-ppm sample (gypsum 50%) was prepared. For the tests, specimens of grout and gypsum without Ag-NPs were also prepared that are named grout 0% and gypsum 0%.

Change of color

The Ag-NP dispersion has a characteristic coloration, close to yellow, due to the plasmon resonance peak. Thus, their incorporation in the studied materials causes a color change. To measure the color variation, the gypsum specimens were photographed with a digital camera (Sony Alpha DSLR A 100), at 20 megapixel resolution, on a stationary table, under the same lighting conditions. These images were transferred to the Photoshop™ software to measure CIELAB color coordinates (McGuire 1992). The parameters *L*, *a,* and *b* determined throughout the specimen were statistically compared by the Kruskal–Wallis test and the difference considered statistically significant when $p < 0.05$. In addition, the UV–visible reflectance spectra were collected on a spectrometer CCD Ocean Optics, model USB-2000.

Minimum inhibitory concentration (MIC)

The MIC of the Ag-NPs was determined for the microorganisms *Staphylococcus aureus* (ATCC 25,923, clinical isolate), *Pseudomonas aeruginosa* (ATCC 25619), *Escherichia coli* (ATCC 25922, clinical isolate) from American Type Culture Collection and filamentous fungus *Aspergillus niger* (IOC/CCFF 3998) from Oswaldo Cruz Institute. The experiment for the components of the specimens grout 0% and grout 100%, gypsum 0% and gypsum 50% was performed against *Staphylococcus aureus* (ATCC 25923). These samples were donated and kept in the collection at the Universidade do Sagrado Coração.

The microdilution test was performed with 96-well microplates (Kasvi®) inoculated with culture medium (MH for bacteria and RPMI for fungi), all values recommended by the Clinical and Laboratory Standards Institute: 10^8 CFU ml^{-1} for bacteria and 5×10^4 UFC ml^{-1} for the fungi (CLSI 2008).

The evaluated concentrations were 428–0.20 µg ml^{-1} for the Ag-NP solutions. Grout 0%, gypsum 0%, grout 100%, and gypsum 50% were also tested.

The antibiotic ampicillin was used as the control substance, since the bacterial strains used are sensitive to its action. The concentration range was 25–0.006 µg ml^{-1}. Amphotericin B was the antifungal used as a control for the *Aspergillus niger* strain. The concentration range was 320–0.15 µg l^{-1}. Control of sterility of the culture media, the antibiotics, nanoparticles, and ultrapure water (Milli-Q) was performed.

For the dilutions, 100 µl of each tested material was applied in the first respective row, followed by serial dilution, discarding the 100 µl of the last well. Thereafter, 100 µl of standard microorganisms was placed in each well. The plates were taken to a bacteriological oven 35 ± 2 °C for 20–24 h (for the bacteria) and 7 days for fungus. For gypsum 0% and 50%, grout 0% and 100% components the same procedure was performed, but only *Staphylococcus aureus* was used.

For evaluation, visual reading with resazurin solution (0.01%) was performed. A volume of 20 µl of solution was added in each well, and plate was then incubated for 1 h at 35 °C in a bacteriological oven. A blue color indicates the absence of viable cells, while a red color, the presence of these cells. The tests were performed in triplicate.

Biofilm tests

Grout 0%, grout 100%, gypsum 0%, and gypsum 50% were tested. The tests were performed with *Staphylococcus aureus* (ATCC 25923). The inoculum suspension was adjusted to 10^7 cel ml^{-1} according to NCCLS, 2015 (Lee et al. 2014; CLSI 2015).

A volume of 2 ml of the standard *Staphylococcus aureus* suspension was added in a 24-well plate. Subsequently, the specimens were placed in contact with microorganism and incubated in a shaker for 90 min at 75 rpm and 37 °C. Later, two consecutive washes with PBS were carried out to discard the unbound cells. The specimens were then transferred to a new plate in which 2 ml of RPMI culture medium was added and then incubated in

a shaker at 75 rpm and 37 °C for 24 h (Zago et al. 2015). After the incubation period and biofilm formation, the specimens were washed again (twice) in PBS, for detachment of unbound cells. For SEM analysis, the biofilm in the samples was fixed in 2 ml of 10% formaldehyde for 1 h at room temperature. After fixation, the specimens were successively immersed in alcohol at concentrations of 70, 85, 100% for 5 min each. After drying, they were stored for scanning electron microscopy (SEM) analysis. The SEM images were taken in Zeiss EVO 50® microscope for all samples with biofilm. As control, an image of the same specimen without biofilm was also recorded.

Aspergilus niger Experiment

The evaluation of specimens against growth of *Aspergillus niger* was also made. We used the Sabouraud Dextrose Agar (Kasvi®) culture medium that was prepared according to the manufacturer's specifications and placed in petri dishes with a thickness of approximately 5 mm. Three specimens of each type were moistened with ultrapure water and placed on the center of petri dish. The filamentous fungus *Aspergillus niger* was then inoculated onto the culture medium. After inoculation, the plates were incubated in a bacteriological oven at 29 °C for 3 days.

Results and Discussion

Synthesis of Ag-NP and specimens

Figure 1a demonstrates the UV–Vis spectrum of the Ag-NP solution. The formation of the Ag-NPs was confirmed by the presence of a plasmonic peak at 390 nm (Khlebtsov 2008; Guidelli et al. 2013; Vesper et al. 2016). Figure 1b shows TEM images of the Ag-NP solution showing small silver particles with a diameter of approximately 20 nm. Particle size distribution obtained by dynamic light scattering (Fig. 1c) is in agreement with size obtained by TEM images.

The color of the grout and gypsum plaster is originally white, and the color of the silver nanoparticles dispersion is yellow due to the plasmon absorption band. After incorporation of the Ag-NPs, the final nanocomposite becomes yellowish, as depicted in Fig. 2. It is well known from the literature that the color and plasmon absorption band of silver nanoparticles are very sensitive to the particles size and particle size distribution, the interparticle distance, as well as the state of agglomeration, and the refractive index of the medium (Guidelli et al. 2016). Therefore, the yellow color of the nanocomposite is a strong evidence that the nanoparticles do not agglomerate after incorporation in the ceramic matrices. To further verify the stability of the Ag-NPs after incorporation into the grout and gypsum matrices, UV–Vis reflectance spectra (Fig. 1d) were obtained for the pure samples of grout and gypsum, as well as for sample containing silver nanoparticles. The presence of the plasmon resonance band around 420 nm in these samples reveals that nanoparticles do not agglomerate after incorporation into the matrices.

The CIELAB color coordinates are displayed in Table 1, where L represents the lightness ($L = 0$ corresponds to black and $L = 100$ to white), a the coordinate at opponent colors red/green axis, and b, in the yellow/blue axis, ranging from −128 to + 127. There was no difference in the L value parameter for all materials tested. However, the comparison between the parameters a and b for each type of material resulted in a statistically significant difference ($p < 0.05$, Kruskal). As shown in the results, the values of b increased as the Ag-NPs concentration increased because of the yellowish coloration of the solution.

Minimum inhibitory concentration (MIC)

The ability of pathogenic bacteria to resist antibiotics is a public health problem (Wright 2000). The choice of bacteria (*S. aureus*, *P. aeruginosa, and E. coli*) and the filamentous fungus (*A. nigger*) in this study is motivated by the large number of pathogens and infestations related to these microorganisms, commonly associated with hospital and residential environments (Beyth et al. 2015; Durán et al. 2016).

The MIC value for the Ag-NP solution found was 26.8 μg ml^{-1} for *Staphylococcus aureus*, *Pseudomonas aeruginosa*, *Escherichia coli*. For ampicillin, the value is 25 μg ml^{-1} for *Escherichia coli* and 0.2 μg ml^{-1} for *Staphylococcus aureus*. Thus, the similar value for *E. coli* and higher (for Ag-NPs) for *S. aureus* is noticed. However, *Pseudomonas aeruginosa* was not inhibited by ampicillin and inhibited by the Ag-NPs, whose MIC was the same as that

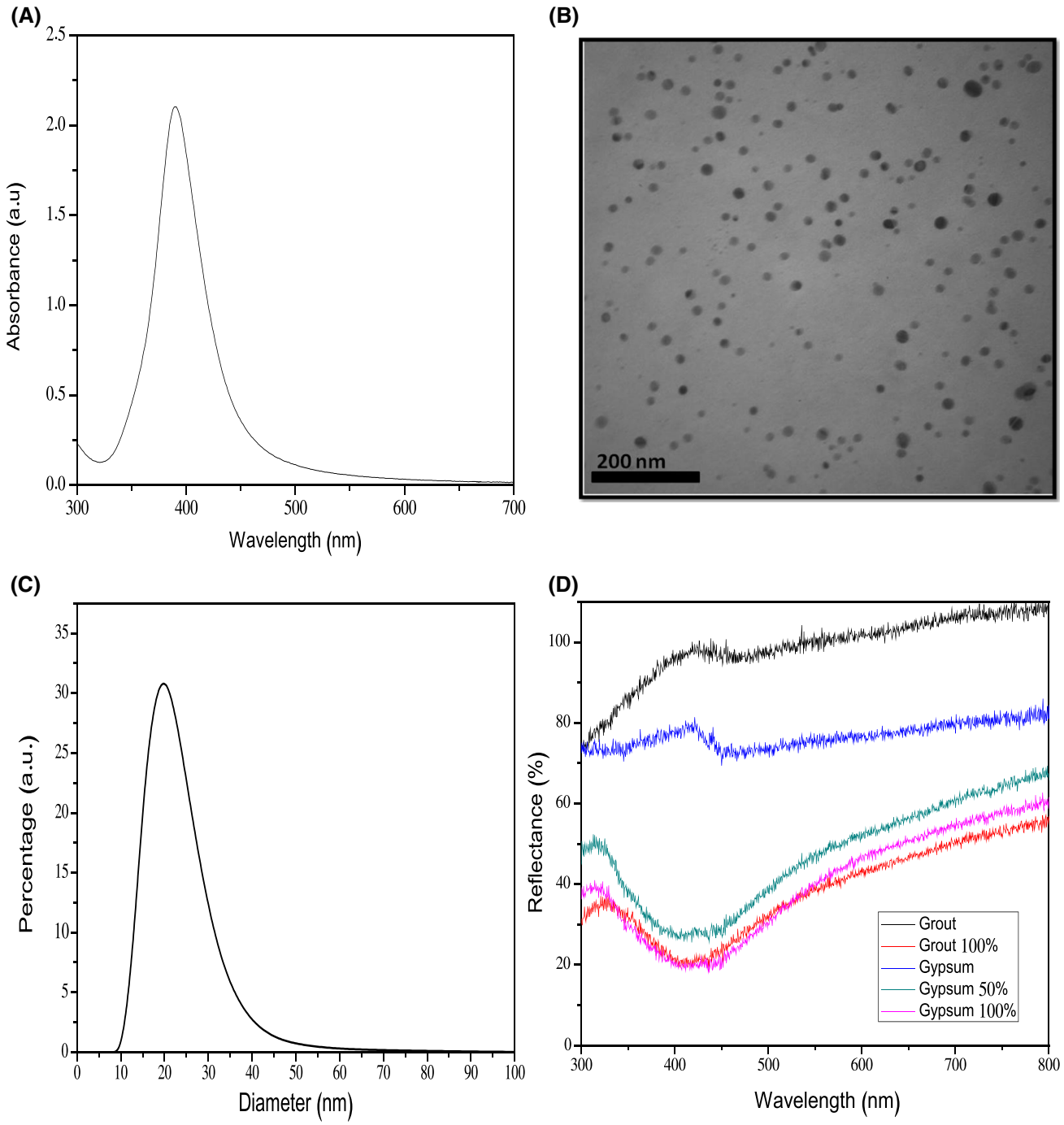

Fig. 1 **a** UV–Vis spectrum of the Ag-NPs. The formation of Ag-NPs was confirmed by the presence of a plasmonic peak at 390 nm. **b** TEM images (JEOL-JEM-CXII-10®) of the Ag-NP solution showing particles with a diameter of approximately 20 nm. **c** Particle size distribution obtained by dynamic light scattering. **d** UV–Vis reflectance spectra of pure grout and gypsum samples and containing silver nanoparticles. The plasmon resonance band around 420 nm reveals that nanoparticles do not agglomerate after incorporation into the matrices

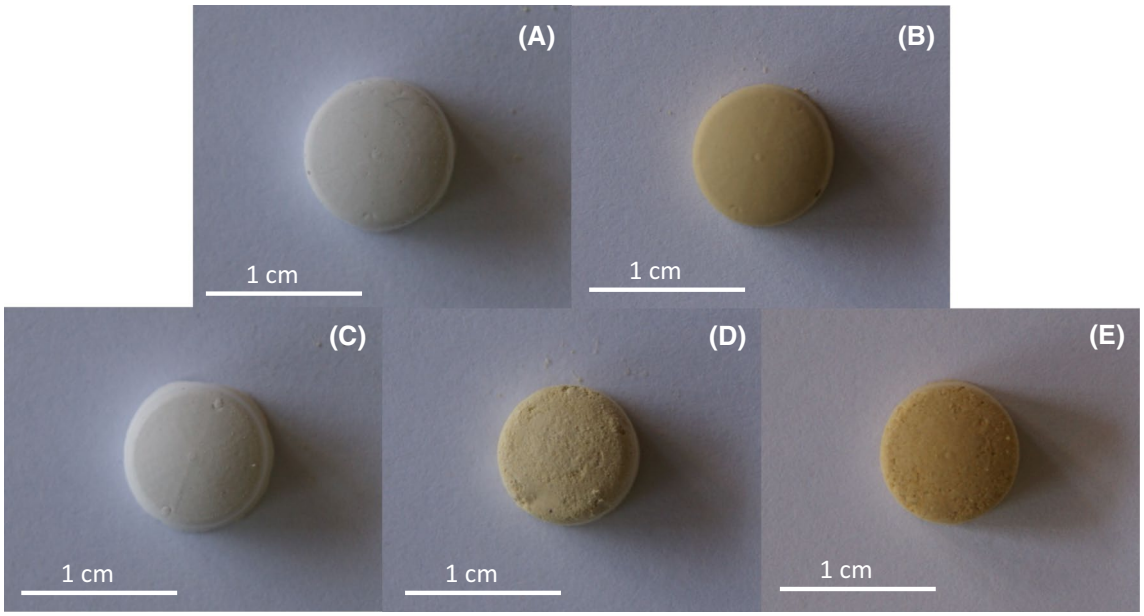

Fig. 2 Photograph of the specimens. **a** Grout 0%; **b** grout 100%; **c** gypsum 0%; **d** gypsum 50%; **e** gypsum 100%

Table 1 The CIELAB color coordinates, where *L* represents the lightness, *a* the coordinate at opponent colors red/green axis, and *b*, in the yellow/blue axis

	L	*a**	*b***
Gypsum 0%	51.9 ± 12.9	1.00 ± 0.01	3.1 ± 0.1
Gypsum 50%	47.1 ± 13.2	4.7 ± 0.07	19.4 ± 0.4
Gypsum 100%	41.2 ± 11.5	12.4 ± 0.2	31.4 ± 0.8
Grout 0%	49.4 ± 13.8	0.83 ± 0.01	2.92 ± 0.05
Grout 100%	41.4 ± 11.6	6.92 ± 0.1	23.3 ± 0.4

* and ** $p < 0.05$ for all comparisons between the same kind of material (Kruskal–Wallis and Student–Newman–Keuls)

found for the other strains. For *A. Niger*, the MIC value for the Ag-NPs found was 428 μg ml^{-1}, higher than for ampicillin B, 160 μg ml^{-1}. Sondi and Salopek-Sondi 2004 found similar value, 50 μg ml^{-1} for *E. coli*.

The MIC test performed with the dilutions of the components of the specimens indicates that test specimens of grout and gypsum, without nanoparticle addition (grout 0% and gypsum 0%), do not exhibit antibacterial activity against *S. aureus*. However, when incorporated with nanoparticles, both grout 100% and gypsum 50% demonstrate inhibition with a MIC that corresponds to 53.3 μg ml^{-1} of Ag-NPs for grout 100% and also 53.3 μg ml^{-1} for gypsum 50%. The specimen gypsum 100% was not tested, but as its concentration is higher than gypsum 50%, it also will exhibit antibacterial activity. As such, these results demonstrate that the media (gypsum and grout) interfere with the Ag-NP antimicrobial activity, since contact with the microorganisms is less when the medium is near the nanoparticles. However, it does not inhibit effectiveness against *S. aureus* remains.

According to Rios and Recio 2005, MICs of compounds below 100 μg ml^{-1} are very interesting because they show low toxicity. A low MIC value, such as the values found, is an important result for the development of coatings containing Ag-NPs, since a small amount will possibly result in the desired antimicrobial effect.

In this work, the MIC values found for Ag-NPs were similar for Gram-positive and Gram-negative bacteria. Fayaz et al. (2010) attribute higher antimicrobial effect in Gram-negative bacteria due to cell membrane characteristics, since Gram-negative bacteria present a thinner cell wall and, therefore, are more sensitive to Ag-NP action. However, the MIC determination methods are different from those applied in this present work.

Dos Santos et al. 2014 and Herman and Herman 2014 attribute the antimicrobial feature of Ag-NPs to the accumulation of Ag in the vicinity of the bacterial membrane,

presenting high permeability through the membrane due to their nanometric dimensions, facilitating cell death. Specifically, for *E. coli*, their action is due to changes in the permeability of the cell membrane that lead to changes in the respiratory process. In *P. aeruginosa*, Ag-NPs cause irreversible bacterial membrane damage, leading to death. In *S. aureus*, both effects occur (Dos Santos et al. 2014). Other studies relate the antimicrobial activity to the reactive oxygen species (ROS) produced by Ag-NPs and indicate a strong relationship with oxidative damage in microbial cells. In addition, ROS has an ability to cause some oxidative damage in cells acting on DNA, RNA, proteins, and lipids (Dos Santos et al. 2014).

Martinez-Castanon et al. 2008 described a different Ag-NPs syntheses using gallic acid in an aqueous chemical reduction and showed that Ag-NPs with smaller sizes are more efficient because they associate with a larger contact area, which allows better contact with cells.

Apergillus niger filamentous fungus growth was inhibited by Ag-NPs, and the MIC value found, 428 μg ml^{-1}, was higher than that of the amphotericin B 160 μg ml^{-1}. Studies related to antifungal activity are also reported in the literature. Swarup et al. 2013 described the action of Ag-NPs against the fungus *Aspergillus niger*, evidencing the improvement in its antifungal activity in relation to the use of $AgNO_3$. Kaur et al. (2012) described antifungal properties of nanoformulated silver/chitosan nanoparticles. The fungal activity against *Rhizoctonia solani, Aspergillus flavus, Alternaria alterneta* of the nanoparticles was observed by the growth inhibition zone. This study suggests the possibility of the use of nanoparticles as protection for plants and crops rather than synthetic fungicides that present high toxicity.

Biofilm and antifungal tests

Biofilms are agglomerates of microorganisms bound to the surface of a material. These agglomerates secrete binding molecules (adhesion proteins) and that, over time, become mature. In the mature phase they become less accessible to antibacterial agents and antibiotics, leading to chronic infections (Watnick and Kolter 2000; Beyth et al. 2015). In this work we verified the influence of Ag-NPs on the formation of *S. aureus* bacterial biofilm.

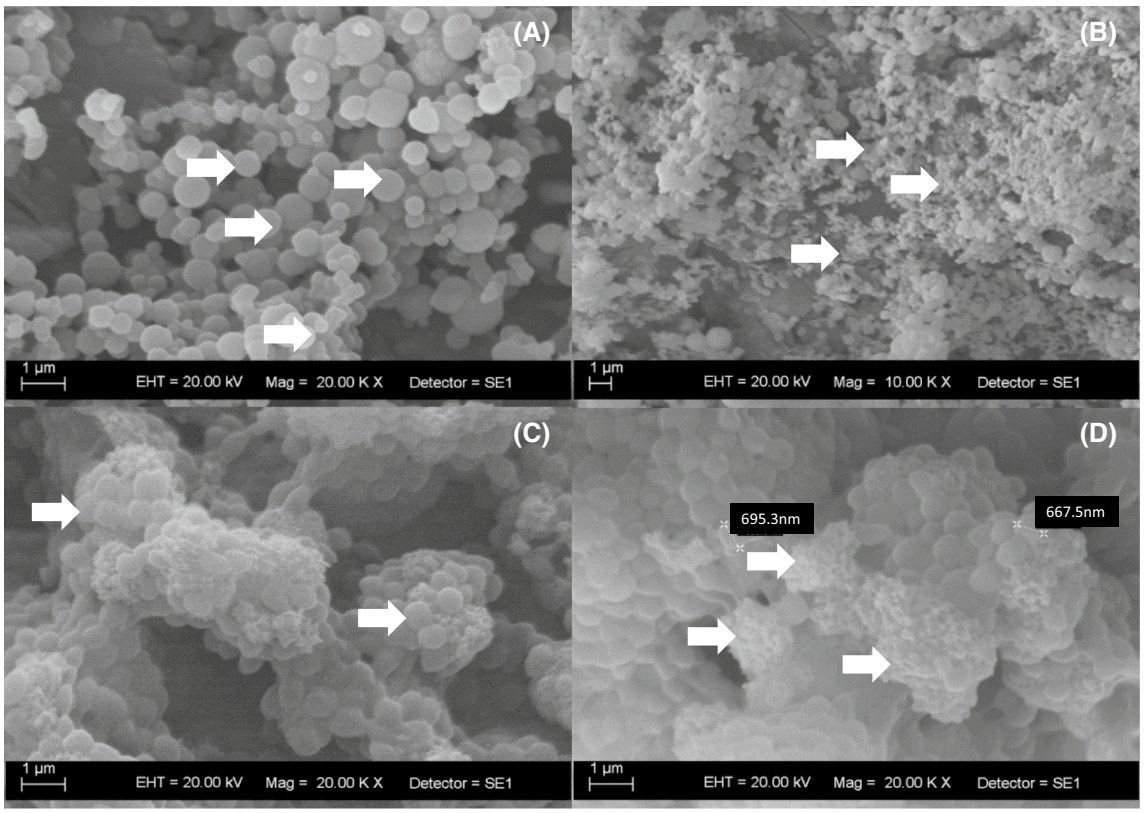

Fig. 3 SEM images of specimens after adhesion of *S. aureus* biofilm. **a** Bacteria (white arrows) in the grout 0% (specimen without Ag-NPs). Scale bar 1 μm, magnification 20 kX. **b** Changes, caused by Ag-NPs, in the morphology of the bacteria in the grout 100% (white arrows). Scale bar 1 μm, magnification 10 kX. **c** In the gypsum 50% amount of biofilm formed is so great (white arrow) that it was impossible to see the surface of the material. Scale bar 1 μm, magnification 20 kX. **d** Gypsum 100%, we can notice the presence of crenate bacteria, however, not on the surface (white arrow). Scale bar 1 μm, magnification 20 kX

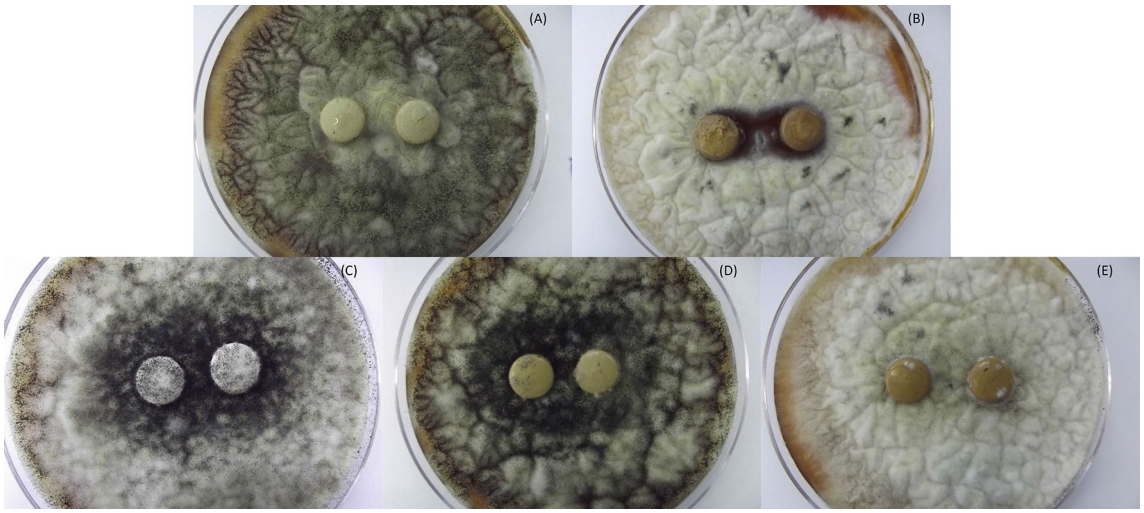

Fig. 4 **a** Grout 0%, without Ag-NPs, the beginning of A. *niger* colonization, with black spots on the surface of the specimen. **b** Grout 100%, the presence of the nanoparticles prevented fungal growth. **c** Gypsum 0% infested with *A. niger* (black spots on surface). **d** Gypsum 50% prevented growth, but did not completely inhibit proliferation; **e** gypsum 100% completely inhibited fungus growth

Figure 3 shows SEM images of specimens after adhesion of the *S. aureus* biofilm. Figure 3a presents the presence of the bacteria (white arrows) in the grout 0% specimen without Ag-NPs and the changes caused by the Ag-NPs in the morphology of the bacteria in the grout 100% (white arrows in Fig. 3b). In the gypsum specimens, because it is an extremely porous material, the amount of biofilm formed is so great (white arrow) that it was impossible to see the surface of the material. There is the possibility of biofilm formation over layers of crenate bacteria on the surface. In the image with the specimens gypsum 50% (3C) and gypsum 100% (3D) we can notice the presence of crenate bacteria; however, they are not on the surface (white arrow).

In the study carried out with the filamentous fungus *Aspergillus niger*, Fig. 4 shows that the specimens with incorporated nanoparticles were effective against the filamentous fungus, avoiding its proliferation. Figure 4a shows grout 0%, without Ag-NPs, in which we can notice the beginning of colonization by A. *niger*, with black spots on the surface of the specimen. In Fig. 4b, there is a yellowish color of the grout incorporated with Ag-NPs (grout 100%) and that the presence of the nanoparticles prevented the growth of the fungus.

Similarly, gypsum 0% (Fig. 4c) is completely infested with *A. niger* (black spots on the surface). Gypsum 50% (Fig. 4d) and gypsum 100% (Fig. 4e) prevented growth, not completely inhibit proliferation, since we can see some black spots on the surface but in a quantity clearly smaller than the gypsum 0%. Herman and Herman 2014 describe the action mechanism of Ag-NPs against *A. niger* as being due to inactivation of sulfhydryl groups in the fungal cell wall with formation of insoluble components.

After use, the common disposal destination of gypsum and grout waste is in a construction landfill. In this location, the material must be properly separated. If recycled, the materials presented in this work will present better properties in relation to those commonly used, since they will not be infested by microorganisms. Even the properties of the remaining wastes that have not been treated can be improved. The impact of Ag-NPs on the environment is the subject of several other research works. Bradford et al. 2009 investigated the impact of Ag-NPs on natural bacterial assemblages in estuarine sediments. They determined that concentrations of up to 1000 μg l^{-1} in water do not cause any changes in bacterial biodiversity of either water or sediment.

Conclusion

In this work, we demonstrate that Ag-NPs can be incorporated to gypsum plaster and grout, maintaining their antimicrobial features improving the material proprieties. These new materials are effective against *S. aureus*, *P. aeruginosa*, *E. coli,* and *A. Niger* and thus can benefit health and the environment, avoiding the proliferation of these microorganisms.

Acknowledgements Authors are grateful to CAPES (Coordination for the Improvement of Higher Education Personnel) for the scholarship granted to one of the authors.

References

Abdelgawad AM, Hudson SM, Rojas OJ (2014) Antimicrobial wound dressing nanofiber mats from multicomponent (chitosan/silver-NPs/polyvinyl alcohol) systems. Carbohydr Polym 100:166–178. https://doi.org/10.1016/j.carbpol.2012.12.043

Ann LC, Mahmud S, Bakhori SKM et al (2014) Antibacterial responses of zinc oxide structures against *Staphylococcus aureus*, *Pseudomonas aeruginosa* and *Streptococcus pyogenes*. Ceram Int 40:2993–3001. https://doi.org/10.1016/j.ceramint.2013.10.008

Bellotti N, Romagnoli R, Quintero C et al (2015) Nanoparticles as antifungal additives for indoor water borne paints. Prog Org Coat 86:33–40. https://doi.org/10.1016/j.porgcoat.2015.03.006

Beyth N, Houri-haddad Y, Domb A et al (2015) Alternative antimicrobial approach: nano-antimicrobial. Materials. https://doi.org/10.1155/2015/246012

Bradford A, Handy RD, Readman JW, Atfield A (2009) Impact of silver nanoparticle contamination on the genetic diversity of natural bacterial assemblages in estuarine sediments. Environ Sci Technol 43:4530–4536. https://doi.org/10.1021/es9001949

Chen Z, Chen ZLG, Liu JZQ (2017) In situ formation of AgNPs on S. cerevisiae surface as bionanocomposites for bacteria killing and heavy metal removal. Int J Environ Sci Technol 14:1635–1642. https://doi.org/10.1007/s13762-017-1261-y

Cheng L, Weir MD, Xu HHK et al (2012) Antibacterial amorphous calcium phosphate nanocomposites with a quaternary ammonium dimethacrylate and silver nanoparticles. Dent Mater 28:561–572. https://doi.org/10.1016/j.dental.2012.01.005

CLSI (2008) Reference method for broth dilution antifungal susceptibility testing of filamentous fungi: approved standard-document M38-A2, 2o edn. Wayne, PA

CLSI (2015) Methods for dilution antimicrobial susceptibility test for bacteria that grow aerobically-document M07-A10 approved standard, 10o edn. Wayne, PA

Dedesko S, Siegel JA (2015) Moisture parameters and fungal communities associated with gypsum drywall in buildings. Microbiome 3:1–15. https://doi.org/10.1186/s40168-015-0137-y

Dos Santos CA, Seckler MM, Ingle AP et al (2014) Silver nanoparticles: therapeutical uses, toxicity, and safety issues. J Pharm Sci 103:1931–1944. https://doi.org/10.1002/jps.24001

Durán N, Durán M, de Jesus MB et al (2016) Silver nanoparticles: A new view on mechanistic aspects on antimicrobial activity. Nanomed Nanotechnol Biol Med 12:789–799. https://doi.org/10.1016/j.nano.2015.11.016

Fayaz AM, Balaji K, Girilal M et al (2010) Biogenic synthesis of silver nanoparticles and their synergistic effect with antibiotics: a study against gram-positive and gram-negative bacteria. Nanomed Nanotechnol Biol Med 6:103–109. https://doi.org/10.1016/j.nano.2009.04.006

Guidelli ÉJ, Kinoshita A, Ramos AP, Baffa O (2013) Silver nanoparticles delivery system based on natural rubber latex membranes. J Nanoparticle Res. https://doi.org/10.1007/s11051-013-1536-2

Guidelli EJ, Ramos AP, Baffa O (2014) Optically stimulated luminescence under plasmon resonance conditions enhances x-ray detection. Plasmonics 9:1049–1056. https://doi.org/10.1007/s11468-014-9713-4

Guidelli EJ, Ramos AP, Baffa O (2016) Silver nanoparticle films for metal enhanced luminescence: toward development of plasmonic radiation detectors for medical applications. Sens Actuat B Chem 224:248–255. https://doi.org/10.1016/j.snb.2015.10.024

Guzman M, Dille J, Godet S (2012) Synthesis and antibacterial activity of silver nanoparticles against gram-positive and gram-negative bacteria. Nanomed Nanotechnol Biol Med 8:37–45. https://doi.org/10.1016/j.nano.2011.05.007

He L, Liu Y, Mustapha A, Lin M (2011) Antifungal activity of zinc oxide nanoparticles against *Botrytis cinerea* and *Penicillium expansum*. Microbiol Res 166:207–215. https://doi.org/10.1016/j.micres.2010.03.003

Herman A, Herman AP (2014) Nanoparticles as antimicrobial agents: their toxicity and mechanisms of action. J Nanosci Nanotechnol. https://doi.org/10.1166/jnn.2014.9054

Jroundi F, Gonzalez-Muñoz MT, Garcia-Bueno A, Rodriguez-Navarro C (2014) Consolidation of archaeological gypsum plaster by bacterial biomineralization of calcium carbonate. Acta Biomater 10:3844–3854. https://doi.org/10.1016/j.actbio.2014.03.007

Kaur P, Thakur R, Choudhary A (2012) An in vitro study of the antifungal activity of silver/chitosan nanoformulations against important seed borne pathogens. Int J Sci Technol Res 1:83–86

Khlebtsov NG (2008) Optics and biophotonics of nanoparticles with a plasmon resonance. Quantum Electron 38:504. https://doi.org/10.1070/QE2008v038n06ABEH013829

Lee K, Lee J-H, Ryu SY et al (2014) Stilbenes reduce Staphylococcus aureus hemolysis, biofilm formation, and virulence. Foodborne Pathog Dis 11:710–717. https://doi.org/10.1089/fpd.2014.1758

Liu Y, Zheng Z, Zara JN et al (2012) The antimicrobial and osteoinductive properties of silver nanoparticle/poly (dl-lactic-co-glycolic acid)-coated stainless steel. Biomaterials 33:8745–8756. https://doi.org/10.1016/j.biomaterials.2012.08.010

Maneerung T, Tokura S, Rujiravanit R (2008) Impregnation of silver nanoparticles into bacterial cellulose for antimicrobial wound dressing. Carbohydr Polym 72:43–51. https://doi.org/10.1016/j.carbpol.2007.07.025

Martinez-Castanon GA, Nino-Martinez N, Martinez-Gutierrez F et al (2008) Synthesis and antibacterial activity of silver nanoparticles with different sizes. J Nanoparticle Res 10:1343–1348. https://doi.org/10.1007/s11051-008-9428-6

McGuire RG (1992) Reporting of objective color measurements. HortScience 27:1254–1255

Morones JR, Elechiguerra JL, Camacho A et al (2005) The bactericidal effect of silver nanoparticles. Nanotechnology 16:2346. https://doi.org/10.1088/0957-4484/16/10/059

Ogar A, Tylko G, Turnau K (2015) Antifungal properties of silver nanoparticles against indoor mould growth. Sci Total Environ 521:305–314. https://doi.org/10.1016/j.scitotenv.2015.03.101

Paschoalino MP, Marcone GPS, Jardim WF (2010) Os nanomateriais e a questão ambiental. Quim Nova 33:421–430. https://doi.org/10.1590/S0100-40422010000200033

Rai M, Yadav A, Gade A (2009) Silver nanoparticles as a new generation of antimicrobials. Biotechnol Adv 27:76–83. https://doi.org/10.1016/j.biotechadv.2008.09.002

Rios JL, Recio MC (2005) Medicinal plants and antimicrobial activity. J Ethnopharmacol 100:80–84. https://doi.org/10.1016/j.jep.2005.04.025

Singh A, Prasad SM (2016) Nanotechnology and its role in agro-ecosystem: a strategic perspective. Int J Environ Sci Technol. https://doi.org/10.1007/s13762-016-1062-8

Sondi I, Salopek-Sondi B (2004) Silver nanoparticles as antimicrobial agent: a case study on *E. coli* as a model for Gram-negative bacteria. J Colloid Interface Sci 275:177–182. https://doi.org/10.1016/j.jcis.2004.02.012

Suresh U, Murugan K, Benelli G et al (2015) Tackling the growing threat of dengue: *Phyllanthus niruri*-mediated synthesis of silver nanoparticles and their mosquitocidal properties against the dengue vector *Aedes aegypti* (Diptera: Culicidae). Parasitol Res 114:1551–1562. https://doi.org/10.1007/s00436-015-4339-9

Swarup R, Mukherjee T, Chakraborty S, Das Kumar T (2013) Biosynthesis, characterisation & antifungal activity of silver

nanoparticles synthesized by the fungus aspergillus foetidus Mtcc8876. Dig J Nanomater Biostruct 8:197–205

Vesper S, Wymer L, Cox D, Dewalt G (2016) Populations of some molds in water-damaged homes may differ if the home was constructed with gypsum drywall compared to plaster. Sci Total Environ 562:446–450. https://doi.org/10.1016/j.scitotenv.2016.04.067

Watnick P, Kolter R (2000) Biofilm, city of microbes. J Bacteriol 182:2675–2679. https://doi.org/10.1128/JB.182.10.2675-2679.2000

Wright GD (2000) Resisting resistance: new chemical strategies for battling superbugs. Chem Biol 7:127–132. https://doi.org/10.1016/S1074-5521(00)00126-5

Xie W, Vu K, Yang G et al (2014) Escherichia coli growth and transport in the presence of nanosilver under variable growth conditions. Environ Technol 35:2306–2313. https://doi.org/10.1080/09593330.2014.902112

Zago CE, Silva S, Sanitá PV et al (2015) Dynamics of biofilm formation and the Interaction between *Candida albicans* and methicillin-susceptible (MSSA) and -resistant *Staphylococcus aureus* (MRSA). PLoS ONE 10:1–15. https://doi.org/10.1371/journal.pone.0123206